Int. J. Solids Structures Vol. 20. No. 5, pp. 429-438, 1984
Printed in Great Britain.

0020-7683/84 $3.00 + .00
Pergamon Press Ltd.

CALCULATED ELASTIC CONSTANTS OF COMPOSITES CONTAINING ANISOTROPIC FIBERS

S. K. Datta
Department of Mechanical Engineering, University of Colorado, Boulder, CO 80309, U.S.A.

and

H. M. Ledbetter and R. D. Kriz
Fracture and Deformation Division, National Bureau of Standards, Boulder, CO 80303, U.S.A.

(*Received* 19 *July* 1982; *in revised form* 9 *February* 1983)

Abstract—By a wave-scattering method, we derive dispersion relationships for waves propagating perpendicular to continuous fibers that are oriented unidirectionally. In the long-wavelength limit one obtains relationships that predict the composite's effective static elastic constants. We compare these relationships with others derived by energy methods to obtain upper and lower bounds of the effective static moduli. We demonstrate them graphically by plotting for graphite-epoxy the predicted composite constants over the full range of fiber volume fractions. We consider the fibers to be anisotropic, but transversely isotropic. Under special conditions, the energy-method upper and lower bounds compare identically with the results of this study. The static properties are, of course, special cases of the more general dispersion relationships. Graphs are given for nine elastic constants: axial and transverse Young's and shear moduli, bulk and plane-strain bulk moduli, and three Poisson's ratios.

1. INTRODUCTION

In recent years, both theory and observation of fiber-reinforced composites have advanced dramatically. Reviews of this subject include those on theory by Hashin[1], Sendeckyj[2], and Walpole[3], and on experiment by Bert[4].

In practice, two types of fiber reinforcement occur: continuous-fiber and short-fiber (chopped-fiber). Most studies consider only the first type, which we consider here.

Most previous studies calculated overall (effective) static elastic constants or bounds of such constants. Interested readers should see [5-14] for relevant studies. Some authors considered wave propagation in fiber-reinforced composites both for fibers in periodic arrays [15, 16] and for fibers distributed randomly[17-19].

Random distributions of identical, long, and parallel fibers form the subject of the present study. We focus on the propagation of plane longitudinal and shear waves propagating perpendicular to the fibers. We use a multiple-scattering approach to obtain a dispersion relationship. This relationship governs both propagation velocity and frequency of the incident wave. We make three simplifying assumptions: (1) random and homogeneous fiber distribution, (2) Lax's quasi-crystalline approximation, (3) wavelength long relative to fiber diameter. In this long-wavelength limit, one obtains effective static elastic constants that agree well with results obtained by other methods. For a graphite-epoxy composite, we consider fibers to be anisotropic, and we obtain elastic constants for all volume fractions.

2. FORMULATION

Consider a system of long circular cylindrical fibers embedded in an infinite matrix. We assume that the matrix is isotropic and homogeneous with Lamé constants λ and μ and mass density ρ and that the fibers are transversely isotropic with the axis of symmetry coincident with the fiber axis. We consider two problems. First, the propagation of shear waves moving perpendicular to the fibers. Here the particle motion is assumed to be parallel to the fibers. This SH-wave problem was considered in [17, 19, 20]. The second problem is that of propagation perpendicular to the fibers with the particle motion also perpendicular to the fibers. Details of the calculation for the first problem are given below. The second problem can be analyzed similarly, except that the algebra is much more complicated because of its vector nature.

2.1 *Shear wave polarized parallel to fiber*

Let the fibers be labeled 1, 2, . . . , N and let (r_i, θ_i) be the polar coordinates of the center 0_i of the ith fiber. The z axis is the fiber axis. We assume that the fibers are identical in geometry and material properties, although for the following analysis this assumption is not necessary. In a customary notation, the fiber elastic constants are denoted by $C_{ij}(i, j = 1\text{–}6)$. Since the fibers are assumed transversely isotropic there are only five independent constants: C_{11}, C_{12}, C_{13}, C_{33} and C_{44}.

For the problem considered in this section, the only elastic properties that enter the calculation are C_{44} and μ. Thus, the analysis follows closely that in [16] and is a special case of that in [19], which deals with elliptical-cross-section inclusions.

Let an SH wave given by

$$u_z^{(i)} = u_0 e^{i(\beta x - \gamma t)}, \quad \beta = \gamma/c_2, \quad c_2 = \sqrt{(\mu/\rho)} \tag{1}$$

be incident on the medium considered. Here u represents particle displacement, c_2 the shear-wave speed in the matrix, and γ the circular frequency.

This incident wave will be scattered by N fibers and the scattered field is given, using rotation in [20], by:

$$u_z^{(s)} = \sum_{i=1}^{N} \hat{T}(\mathbf{r}_i) u_z^E(\mathbf{r}|\mathbf{r}_i) \tag{2}$$

where u_z^E is the field near the ith scatterer and will be called the exciting field[20]. The operator $\hat{T}(\mathbf{r}_i)$ operating on u_z^E gives the scattered field due to the ith scatterer. It is well known, see [20], that $\hat{T}u_z^E$ can be written

$$\hat{T}(\mathbf{r}_i) u_z^E(\mathbf{r}|\mathbf{r}_i) = \sum_{n=0}^{\infty} \mu_n [A_{in}^1 \cos(n\phi_i) + A_{in}^2 \sin(n\phi_i)] H_n(\beta R_i) \tag{3}$$

where $\mu_0 = 1/2$, $\mu_n = 1$ $(n > 0)$, R_i and ϕ_i are shown in Fig. 1, and H_n and J_n are Hankel and Bessel functions of the first kind. The coefficients A_{in}^1 and A_{in}^2 depend on the boundary conditions at the surface of the fibers and are not generally obtainable in closed form. Equation (2) can be rewritten as

$$u_z^{(s)} = \sum_{n=0}^{\infty} \mu_n [A_{in}^1 \cos(n\phi_i) + A_{in}^2 \sin(n\phi_i)] H_n(\beta R_i) + \sum_{j \neq i}^{\infty} \sum_{n=0}^{\infty} \mu_n [a_{jn}^1 \cos(n\phi_i) + a_{jn}^2 \sin(n\phi_i)] J_n(\beta R_i) \tag{4}$$

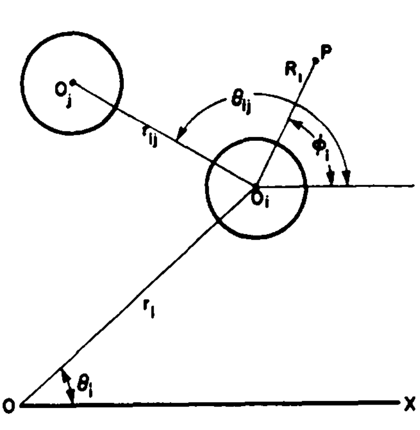

Fig. 1.

where

$$a^1_{jn} = \sum_{m=0}^{\infty} \mu_m[(-1)^m(A_{j,n+m} + (-1)^n A_{j,-n+m})\, e^{im\theta_{ij}} + (A_{j,n-m} + (-1)^n A_{j,-n-m})\, e^{-im\theta_{ij}}]H_m(\beta r_{ij}) \quad (5)$$

$$a^2_{jn} = \sum_{m=0}^{\infty} i\mu_m[(-1)^m(A_{j,n+m} - (-1)^n A_{j,-n+m})\, e^{im\theta_{ij}} + (A_{j,n-m} - (-1)^n A_{j,-n-m})\, e^{-im\theta_{ij}}]H_m(\beta r_{ij}) \quad (6)$$

where

$$A_{ip} = \frac{1}{2}(A^1_{ip} - iA^2_{ip}) \quad (-1)^p A_{i,-p} = \frac{1}{2}(A^1_{ip} + A^2_{ip}).$$

The boundary conditions on the ith scatterer are:

$$(u_z^{(i)} + u_z^{(s)})|_{R_i=a} = u'_z|_{R_i=a} \quad (7)$$

and

$$\mu \frac{\partial}{\partial R_i}(u_z^{(i)} + u_z^{(s)})|_{R_i=a} = C_{44}\frac{\partial u'_z}{\partial R_i}\bigg|_{R_i=a}. \quad (8)$$

Here u'_z is the field within the ith scatterer and can be expanded in the form:

$$u'_z = \sum_{n=0}^{\infty} \mu_n[A'^1_{in}\cos(n\phi_i) + A'^2_{in}\sin(n\phi_i)]J_n(\beta R_i) \quad (9)$$

where

$$0 \le R_i < a.$$

Substituting (1), (4), and (9) into (7) and (8) yields a set of equations for the unknowns A^1_{in}, A^2_{in}, A'^1_{in}, and A'^2_{in}. The solution for A^1_{in} and A^2_{in} can be written as

$$A^1_{in} = \hat{T}^{1\nu}_{nm}\alpha^{\nu}_{im},\ A^2_{in} = \hat{T}^{2\nu}_{nm}\alpha^{\nu}_{im} \quad (10)$$

where

$$\alpha^1_{im} = 2u_0 i^m\, e^{i\beta x_i} + \sum_{j\neq i} a^1_{jm},\ \alpha^2_{im} = \sum_{j\neq i} a^2_{jm}.$$

The repeated index implies summation over that index. It can be shown that

$$\hat{T}^{1\nu}_{nm} = iC_n\delta_{nm}\delta_{1\nu} \quad \hat{T}^{2\nu}_{nm} = iC_n\delta_{nm}\delta_{2\nu} \quad (\text{no sum on } n) \quad (11)$$

where

$$C_n = \frac{\mu J_n(\beta'_a a)\frac{\partial}{\partial a}J_n(\beta a) - C_{44}J_n(\beta a)\frac{\partial}{\partial a}J_n(\beta' a)}{C_{44}H_n(\beta a)\frac{\partial}{\partial a}J_n(\beta' a) - \mu J_n(\beta' a)\frac{\partial}{\partial a}J_n(\beta a)}$$

$$\beta' = \gamma/c'_2, \quad c'_2 = \sqrt{(C_{44}/\rho')}.$$

Similar expressions can be obtained for A'^1_{in} and A'^2_{in}.

Having the formal expressions for the scattered field we now proceed to take ensemble averages. For this purpose we assume a homogeneous fiber distribution. In this case the position of a single fiber is equally probable within the region S, the total specimen area. Hence its distribution, p, is uniform with density:

$$p(\mathbf{r}_i) = \begin{cases} 1/S, \mathbf{r}_i \in S; \\ 0, \mathbf{r}_i \notin S. \end{cases} \tag{12}$$

Having the center of the ith fiber at 0_i the conditional probability density of the jth fiber at $\mathbf{r}_j$ is:

$$p(\mathbf{r}_j|\mathbf{r}_i) = \begin{cases} 1/S(1 - f(\mathbf{r}_{ij})), & \mathbf{r}_j \in S \\ 0, & \mathbf{r}_j \notin S \end{cases} \tag{13}$$

where the pair-correlation function $f(r_{12})$ has the property:

$$f(\mathbf{r}_{ij}) = \begin{cases} 1, & \mathbf{r}_{ij} < 2a \\ \text{approaches 0 as } \mathbf{r}_{ij} \text{ approaches } \infty. \end{cases} \tag{14}$$

For the purpose of this study we assume that $f(\mathbf{r}_{ij}) = 0$, which is asymptotically valid for small fiber concentrations. Neglecting $f(\mathbf{r}_{ij})$ implies no pair correlations, an assumption discussed by Bose and Mal [18]. Equation (13) implies an isotropic distribution. Together with the quasi-crystalline approximation made below in (17), this has been shown [21] to lead to optimum bounds. By optimum we mean with respect to the Hashin–Shtrikman variational principle [22] for isotropic distribution of spherical inclusions in an isotropic matrix. Equation (14), often called the "well-stirred" approximation, becomes invalid at high concentrations. Nevertheless, we expect from the discussion in [21] that the present study will lead to the general bounds [23, 24] in the long-wavelength limit.

Taking now the ensemble average of the total field u_z we obtain:

$$\begin{aligned} \langle u_z \rangle = (1 - C)\, e^{i\beta x} + n_0 \int_{|\mathbf{r}-\mathbf{r}_i|>a} d\mathbf{r}_i \hat{T}(\mathbf{r}_i) < u_z^E(\mathbf{r}|\mathbf{r}_i) > \\ - n_0^2 \int_{|\mathbf{r}-\mathbf{r}_i|>a} d\mathbf{r}_i \int_{|\mathbf{r}_j-\mathbf{r}_i|>2a} d\mathbf{r}_j \hat{T}(\mathbf{r}_j) \langle u_z^E(\mathbf{r}|\mathbf{r}_j, \mathbf{r}_i)\rangle \\ + n_0 \int_{|\mathbf{r}-\mathbf{r}_i| \le a} d\mathbf{r}_i T'(\mathbf{r}_i) \langle u_z^E(\mathbf{r}|\mathbf{r}_i)\rangle. \end{aligned} \tag{15}$$

where n_0 is the number density of the fibers and $C = n_0 \pi a^2$.

The average exciting field on the scatterer at $\mathbf{r}_i$ is given by:

$$\langle u_z^E(\mathbf{r}|\mathbf{r}_i)\rangle = u_0\, e^{i\beta x} + n_0 \int_{|\mathbf{r}_j-\mathbf{r}_i|>2a} d\mathbf{r}_j \hat{T}(\mathbf{r}_j) \langle u_z^E(\mathbf{r}|\mathbf{r}_j, \mathbf{r}_i)\rangle. \tag{16}$$

It is seen that the first partial average of the exciting field at $\mathbf{r}_i$ depends on the second partial average of the same. An equation for the second partial average will depend on the third, and so on.

This hierarchy is terminated here by making the quasi-crystalline approximation that requires

$$\langle u_z^E(\mathbf{r}|\mathbf{r}_j, \mathbf{r}_i)\rangle = \langle u_z^E(\mathbf{r}|\mathbf{r}_i)\rangle. \tag{17}$$

This makes (16) an integral equation for $\langle u_z^E(\mathbf{r}|\mathbf{r}_i)\rangle$.

To solve this equation it may be assumed that

$$\langle u_z^E(\mathbf{r}|\mathbf{r}_i)\rangle = \sum_{n=0}^{\infty} \mu_n [a_{in}^1 \cos(n\phi_i) + b_{in}^1 \sin(n\phi_i)] J_n(\beta R_i). \tag{18}$$

Then from (3)

$$\hat{T}(\mathbf{r}_i)\langle u_z^E(\mathbf{r}|\mathbf{r}_i)\rangle = \sum_{n=0}^{\infty} \mu_n[A_{jn}^1 \cos(n\phi_j) + A_{jn}^2 \sin(n\phi_j)]H_n(\beta R_j). \tag{19}$$

Thus we obtain:

$$\begin{aligned} a_{ip}^1 = 2u_0 i^p e^{i\beta x_i} + n_0 \int_{|\mathbf{r}_i-\mathbf{r}_j|>2a} d\mathbf{r}_j \sum_{n=0}^{\infty} \frac{1}{2}\mu_n \{(\hat{T}_{nq}^{1\nu} - \hat{T}_{nq}^{2\nu}) \\ \times [H_{p-n}(\beta r_{ij})\, e^{-i(p-n)\theta_{ij}} + (-1)^n H_{p+n}\, e^{i(p+n)\theta_{ij}}] \\ + (\hat{T}_{nq}^{1\nu} + i\, T_{nq}^{2\nu})[H_{p-n}\, e^{i(p-n)\theta_{ij}} + (-1)^n H_{p+n}\, e^{i(p+n)\theta_{ij}}]\}\, a_{jq}^{\nu} \end{aligned} \tag{20}$$

$$\begin{aligned} a_{ip}^2 = n_0 \int_{|\mathbf{r}_i-\mathbf{r}_j|>2a} d\mathbf{r}_j \sum_{n=0}^{\infty} \frac{1}{2}\mu_n \{(\hat{T}_{nq}^{1\nu} - i\,\hat{T}_{nq}^{2\nu})[H_{p-n}\, e^{-i(p-n)\theta_{ij}} \\ - (-1)^n H_{p+n}\, e^{i(p+n)\theta_{ij}}] - (\hat{T}_{nq}^{1\nu} + i\hat{T}_{nq}^{2\nu})[H_{p-n}\, e^{i(p-n)\theta_{ij}} \\ - (-1)^n H_{p+n}\, e^{-i(p+n)\theta_{ij}}]\}\, a_{jq}^{\nu}. \end{aligned} \tag{21}$$

Equations (20) and (21) define a pair of integral equations in the unknowns a_{ip}^1 and a_{ip}^2. If it is assumed that an effective plane wave is propagating through the medium, then a solution for a_{ip}^{ν} may be assumed in the form

$$a_{ip}^{\nu} = X_p^{\nu}\, e^{i\beta^* x_i} \tag{22}$$

where γ/β^* is the wave velocity of the plane wave.

The coefficients X_p^{ν} form a set of linear homogeneous algebraic equations. These are:

$$X_p^1 = -\frac{2\pi n_0 a}{\beta^{*2}-\beta^2} \sum_{n=0}^{\infty} \mu_n\, i^{p-n} \hat{T}_{nq}^{1\nu} X_q^{\nu}(\Delta_{p-n} + \Delta_{p+n}) \tag{23}$$

$$X_p^2 = -\frac{2\pi n_0 a}{\beta^{*2}-\beta^2} \sum_{n=0}^{\infty} \mu_n\, i^{p-n} \hat{T}_{nq}^{2\nu} X_q^{\nu}(\Delta_{p-n} + \Delta_{p+n}) \tag{24}$$

where

$$\Delta_m = \left[\frac{\partial}{\partial a} H_m(2\beta a)\right] J_m(2\beta^* a) - \left[\frac{\partial}{\partial a} J_m(2\beta^* a)\right] H_m(2\beta a). \tag{25}$$

Because of relationships (11), X_p^1 and X_p^2 are uncoupled. However, for noncircular-cross-section fibers they are coupled. The dispersion equation is obtained by equating the coefficients of X_p^1 and X_p^2 to zero. For an arbitrary wavenumber the dispersion equation is rather complicated. We can approximate this equation by assuming that βa is small; this means the wavelength is long compared to the fiber diameter. For small βa and $\beta' a$ the following relationships can be obtained, which are correct to order $(\beta a)^2$:

$$C_0 = \frac{\pi}{4}(\beta a)^2(\rho/\rho' - 1), \quad C_1 = \frac{\pi}{4}(\beta a)^2 \frac{C_{44} - \mu}{C_{44} + \mu} \tag{26}$$

$$C_m = 0 \text{ for } m \geq 2$$

and

$$\Delta_m = \left(\frac{2i}{\pi a}\right)\left(\frac{\beta^*}{\beta}\right)^{|m|}. \tag{27}$$

Substituting (26) into (11), and then into (23), and using (27) one obtains:

$$i^p X_p{}^1 = \frac{2\pi n_0 a}{\beta^{*2}-\beta^2}\sum_{n=0}^{\infty}\mu_n\left(\frac{2}{\pi a}\right) i^{-n} X_n{}^1 C_n\left\{\left(\frac{\beta^*}{\beta}\right)^{|p-n|}+\left(\frac{\beta^*}{\beta}\right)^{p+n}\right\}. \tag{28}$$

Because of (26) the infinite series can be terminated after $n = 1$. This yields two simultaneous homogeneous equations in $X_0{}^1$ and $X_1{}^1$. Equating the determinant of the coefficients to zero gives the dispersion relationship:

$$\left(\frac{\beta^*}{\beta}\right)^2 = [1 + C(\rho'/\rho - 1)]\ \frac{1 - C(m-1)/(m+1)}{1 + C(m-1)/(m+1)} \tag{29}$$

where $m = C_{44}/\mu$ and C is the fiber volume fraction.

Defining the average density as

$$\rho^* = \rho[1 + C(\rho'/\rho - 1)] \tag{30}$$

and

$$\beta^* = \gamma/c_2^*, \quad c_2^* = \sqrt{(\mu_{LT}/\rho^*)} \tag{31}$$

where μ_{LT} is the effective axial shear modulus, one obtains:

$$\frac{\mu_{LT}}{\mu_m} = \frac{1 + C(m-1)/(m+1)}{1 - C(m-1)/(m+1)} \tag{32}$$

where m is the ratio of fiber and matrix shear moduli (μ'_{LT}/μ_m).

Equation (32) was obtained by Hashin and Rosen[25] using the composite cylinder assemblage (CCA) model. The expression for μ_{LT} obtained from (32) coincides with the lower (upper) bound when the fiber shear modulus, μ'_{LT}, is larger (smaller) than the matrix shear modulus, μ_m.

2.2 *Longitudinal and shear waves polarized perpendicular to fiber*

Propagation of longitudinal and shear waves polarized transverse to the fibers was studied in [18] using the same approach outlined above. It was shown that if βa and αa were assumed small then the dispersion relationships reduce to effective longitudinal and shear moduli transverse to the fibers. These are:

$$\frac{C_{11}}{\lambda_m + 2\mu_m} = \frac{1 - CP_2(1-\beta^2/\alpha^2) - 2c^2 P_0 P_2}{(1 + CP_0)[1 + CP_2(1+\beta^2/\alpha^2)]} \tag{33}$$

$$\frac{\mu_{TT}}{\mu_m} = 1 + \frac{2C(\mu'_{TT}-\mu_m)(\lambda_m + 2\mu_m)}{2\mu_m(\lambda_m + 2\mu_m) + (1-C)(\lambda_m + 3\mu_m)(\mu'_{TT} - \mu_m)} \tag{34}$$

where

$$P_0 = -\frac{K'_T - (\lambda_m + \mu_m)}{K'_T + \mu_m}, \quad P_2 = -\frac{(\mu'_{TT} - \mu_m)\mu_m}{\mu'_{TT}(\lambda_m + 3\mu_m) + \mu_m(\lambda_m + \mu_m)}$$

$$\alpha^2 = \gamma^2/c_1{}^2, \quad c_1 = \sqrt{((\lambda_m + 2\mu_m)/\rho)}.$$

The effective transverse plane-strain bulk modulus, K_T, can be obtained from eqns (33) and (34) as:

$$K_T = \lambda_m + \mu_m + (\lambda_m + 2\mu_m)\frac{C(K'_T - \lambda_m - \mu_m)}{(1-C)K'_T + C\lambda_m + (1+C)\mu_m} \tag{35}$$

where K'_T is the fiber plane-strain bulk modulus and the matrix Lamé constants are λ_m and μ_m.

Equation (35) is the same as derived by Hashin and Rosen[25] using the CCA model. However, the CCA model does not yield an expression for the effective transverse shear modulus. Instead, bounds for the transverse shear modulus are noted. Expression (34) for μ_{TT} is identical to the general lower (upper) bound derived for arbitrary phase geometry[23, 24] if μ'_{TT} and K'_T are larger (lower) than μ_m and K_m, respectively, where $K_m = \lambda_m + \mu_m$ is the plane-strain bulk modulus of the matrix.

Knowing the expression for K_T one can predict the effective longitudinal Young's modulus and Poisson's ratio using relationships derived by Hill[23]. When both fiber and matrix phases are transversely isotropic, Hill shows that:

$$E_L = E_m(1-C) + E'_L C + \frac{4C(1-C)(\nu'_{LT} - \nu_m)^2}{(1-C)/K'_T + C/K_m + 1/\mu_m} \tag{36}$$

$$\nu_{LT} = \nu_m(1-C) + \nu'_{LT} C + \frac{C(1-C)(\nu'_{LT} - \nu_m)(1/K_m - 1/K'_T)}{(1-C)/K'_T + C/K_m + 1/\mu_m} \tag{37}$$

where E'_L and ν'_{LT} are the axial Young's modulus and axial Poisson's ratio of the fiber. The quantities subscripted with m designate the isotropic matrix properties.

For a unidirectional fibrous composite with transversely isotropic fibers, this completes the derivation of the five independent effective elastic properties: K_T, E_L, ν_{LT}, μ_{TT}, μ_{LT}. Other elastic properties of physical significance can be calculated from the five effective properties. For instance, assuming isotropy in the transverse plane, T, the Poisson's ratio, ν_{TT}, and the Young's modulus, E_T, can be calculated from the isotropic relationships. Thus,

$$E_T = \frac{4K_T\mu_{TT}}{K_T + \psi\mu_{TT}} \tag{38}$$

$$\nu_{TT} = \frac{K_T - \psi\mu_{TT}}{K_T + \psi\mu_{TT}} \tag{39}$$

where

$$\psi = 1 + \frac{4K_T\nu_{LT}^2}{E_L}.$$

The remaining Poisson's ratio, ν_{TL}, is calculated from the relationship obtained from the elastic-compliance symmetry condition:

$$\nu_{TL} = \nu_{LT}E_T/E_L. \tag{40}$$

If the composite behaves transversely isotropic with the unique symmetry axis along x_3, then the elastic-stiffness constants, C_{ij}, can be computed from

$$C_{11} = C_{22} = K_T + \mu_{TT} \tag{41}$$

$$C_{33} = E_L + 2\nu_{LT}C_{13} \tag{42}$$

$$C_{44} = C_{55} = \mu_{LT} \tag{43}$$

$$C_{12} = K_T - \mu_{TT} \tag{44}$$

$$C_{13} = C_{23} = 2\nu_{LT}K_T \tag{45}$$

$$C_{66} = (C_{11} - C_{12})/2 = \mu_{TT}. \tag{46}$$

One can also calculate the bulk modulus, B, from

$$B=\frac{1}{9}\sum_{i,j=1,2,3} C_{iijj}=\{E_L+4K_T[1+\nu_{LT}(\nu_{LT}+2)]\}/9. \tag{47}$$

RESULTS AND DISCUSSION

The effect of fiber volume fraction, C, on the predicted elastic constants can now be demonstrated given the isotropic matrix properties and the transversely isotropic fiber properties. The matrix and fiber elastic constants, listed in Table 1, were obtained from [26] where the fiber elastic properties were extrapolated from experiments of Dean and Turner[27] using the transversely isotropic relations derived by Hashin[1]. This extrapolation of fiber properties was done with the correction $\beta_2=K_T'/(K_T'+2\mu_{TT}')$ noted in [28]. The elastic properties (ν_{TT}, ν_{TL}, ν_{LT}, μ_{TT}, E_T, μ_{LT}, E_L, K_T, B) are shown in Figs 2–5.

As noted above, the curves for K_T, μ_{TT}, and μ_{LT} coincide with the general lower bounds[28] for the particular constituent properties considered here. Of the nine elastic constants shown in Figs. 2–5, E_L best fits a simple rule of mixtures. (The correction term in (36) can be neglected.) Both B and ν_{LT} come close to fitting this rule; μ_{TT}, K_T, and E_T do not differ dramatically from linearity; but μ_{TT}, ν_{TT}, and ν_{TL} do so differ. Except for ν_{TT} and E_T all deviations from linearity are negative, that is, the curves are concave. The ν_{TT} curve is convex. The E_T curve is convex at low fiber fractions and concave at high. This reflects the abrupt rise of ν_{TT} at low fiber fractions combined with the slow, steady rise of μ_{TT}. For those constants that differ strongly from a rule of mixtures, both ν_{TT} and ν_{TL} are fiber-property dominated while μ_{LT} tends to be matrix-property dominated. The latter represents, of course, shear in the fiber direction.

Table 1. Matrix and fiber elastic constants, ref. [26]

	E (GPa)	G (GPa)	ν
Epoxy	5.35	1.95	0.353
Graphite fiber (L)	232.0	24.0	0.290
Graphite fiber (T)	15.0	5.02	0.490

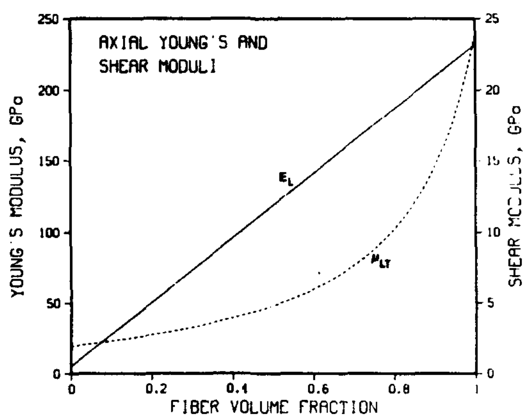

Fig. 2.

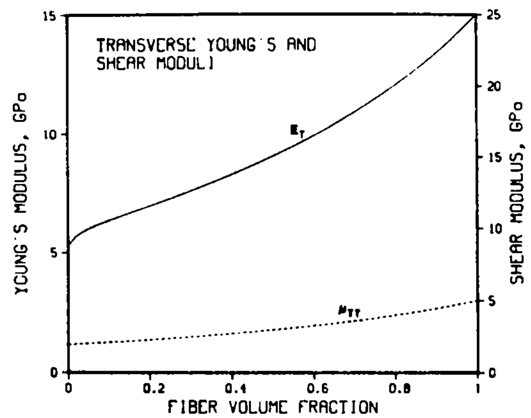

Fig. 3.

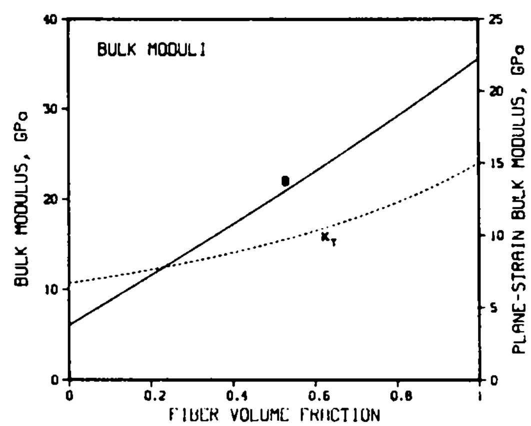

Fig. 4.

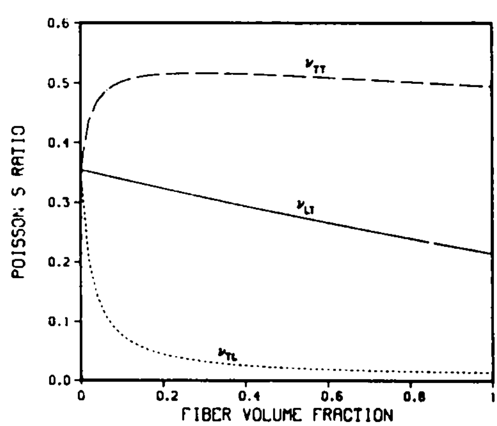

Fig. 5.

4. CONCLUSIONS

Using a multiple-scattering approach, effective elastic constants of a graphite-fiber-reinforced epoxy composite were derived in this study. Graphite fibers were assumed to be anisotropic, but transversely isotropic. It was shown that the composite can be characterized as a transversely isotropic medium. All five elastic constants characterizing the composite were calculated. These elastic constants coincide with the general lower bounds of those obtained in [1, 23, 24] using energy methods.

Acknowledgement—Composites studies of H.M.L. and R.D.K. are supported mainly by the U.S. Department of Energy, Office of Fusion Energy.

REFERENCES

1. Z. Hashin, Theory of fiber-reinforced materials. NASA Rep. CR-1974 (1972).
2. G. P. Sendeckyj, Elastic behavior of composites. In *Composite Materials*, Vol. 2, pp. 45–83. Academic Press, New York (1974).
3. L. J. Walpole, Elastic behavior of composite materials: theoretical fundamentals. In *Advances in Applied Mechanics*, Vol. 21, pp. 169–242. Academic Press, New York (1981).
4. C. W. Bert, Experimental characterization of composites. In *Composite Materials*, Vol. 8, pp. 73–133. Academic Press, New York (1975).
5. J. J. Hermans, The elastic properties of fiber reinforced materials when the fibers are aligned. *Proc. Koninklijke Netherlandse Akademie van Wetenschappen* **70B**, 1–9 (1967).
6. J. M. Whitney, Elastic moduli of unidirectional composites with anisotropic filaments. *J. Compos. Mater.* **1**, 188–193 (1967).
7. J. M. Bloom and D. F. Adams, Axial loading of a unidirectional composite—anisotropic filaments. *J. Compos. Mater.* **3**, 186–188 (1969).
8. M. D. Heaton, A calculation of the elastic constants of a unidirectional composite containing transversely isotropic fibres. *J. Phys. D* **3**, 672–676 (1970).
9. C. H. Chen and S. Cheng, Mechanical properties of anisotropic fiber reinforced composites. *J. Appl. Mech.* **37**, 186–189 (1970).
10. C. H. Chen, Rectangular or square array fibrous composite with anisotropic or isotropic filament. *J. Appl. Mech.* **38**, 710–712 (1971).
11. E. Behrens, Elastic constants of fiber-reinforced composites with transversely isotropic constituents. *J. Appl. Mech.* **38**, 1062–1065 (1971).
12. F. Ya. Bulavs, Ya. V. Auzukalns and A. M. Skudra, Deformation characteristics of plastics reinforced with high-modulus anisotropic fibers. *Polymer Mech.* **8**, 545–552 (1972).
13. H. T. Yeh, Variational bounds of unidirectional fiber reinforced composites. *J. Appl. Phys.* **44**, 662–665 (1973).
14. G. A. Ermakov, A. G. Fokin and T. D. Shermergor, Effective moduli of elasticity for materials reinforced by anisotropic fibers. *Mech. Solids* **9**, 98–104 (1974).
15. J. D. Achenbach, Generalized continuum theories for directionally reinforced solids. *Arch. Mech.* **28**, 257–278 (1976).
16. M. Hlavacek, A continuum theory of fiber-reinforced composites. *Int. J. Solids Structures* **9**, 1075–1085 (1973).
17. S. K. Bose and A. K. Mal, Longitudinal shear waves in a fiber-reinforced composite. *Int. J. Solids Structures* **9**, 1075–1085 (1973).
18. S. K. Bose and A. K. Mal, Elastic waves in a fiber-reinforced composite. *J. Mech. Phys. Solids* **22**, 217–229 (1974).
19. S. K. Datta, Propagation of SH-waves through a fiber-reinforced composite—elliptic cylindrical fibers. *J. Appl. Mech.* **42**, 165–175 (1975).
20. S. K. Datta, Scattering by a random distribution of inclusions and effective elastic properties. In *Continuum Model of Discrete Systems, Solid Mechanics Study Series No.* 12, pp. 111–127. University of Waterloo Press (1978).
21. J. R. Willis, Variational and related methods for the overall properties of composites. In *Advances in Applied Mechanics*, Vol. 21, pp. 1–78. Academic Press, New York (1981).
22. Z. Hashin and S. Shtrikman, On some variational principles in anisotropic and nonhomogeneous elasticity. *J. Mech. Phys. Solids* **10**, 335–342 (1964).
23. R. Hill, Theory of mechanical properties of fibre-strengthened materials—I. Elastic behaviour. *J. Mech. Phys. Solids* **12**, 199–212 (1964).
24. Z. Hashin, On elastic behaviour of fibre-reinforced materials of arbitrary phase geometry. *J. Mech. Phys. Solids* **13**, 119–134 (1965).
25. Z. Hashin and B. W. Rosen, The elastic moduli of fiber-reinforced materials. *J. Appl. Mech.* **31**, 223–232 (1964).
26. R. D. Kriz and W. W. Stinchcomb, Elastic moduli of transversely isotropic graphite fibers and their composites. *J. Exper. Mech.* **19**, 41–49 (1979).
27. G. D. Dean and P. Turner, The elastic properties of carbon fibers and their composites. *Composites* **4**, 174–180 (1973).
28. Z. Hashin, Analysis of properties of fiber composites with anisotropic constituents. *J. Appl. Mech.* **46**, 546–550 (1979).